Rapid Loop Dynamics of *Yersinia* Protein Tyrosine Phosphatases†

Laura J. Juszczak,‡ Zhong-Yin Zhang,§ Li Wu,§ David S. Gottfried,‡ and Daniel D. Eads*,‡

Albert Einstein College of Medicine, Yeshiva University, Bronx, New York 10461

Received August 30, 1996; Revised Manuscript Received January 2, 1997⊗

ABSTRACT: The *Yersinia* protein tyrosine phosphatases (PTPase) contain a single and invariant tryptophan (W354) located at one of the hinge positions of the flexible loop (WpD loop), which is essential for catalysis. The wild-type *Yersinia* PTPase and an active site mutant in which the esential Cys 403 has been replaced by serine (C403S) have been examined using both time-resolved fluorescence anisotropy and steady-state UV resonance Raman (UVRR) spectroscopies. Both enzymes were examined with and without the bound inhibitor arsenate. The UVRR spectra indicate that in solution the ligand-free, wild-type PTPase exists as an equilibrium mixture of two tryptophan rotamer structures with $\chi^{2,1}$ dihedral angles of −4° and −90°. The two rotamers have been attributed to the presence of both "closed" and "open" WpD loop conformers of the ligand-free enzyme. Conversely, the UVRR spectra of the arsenate-ligated, wild-type PTPase and of ligand-free and arsenate-ligated C403S PTPase contain a single W3 band which is correlated to the −4° rotamer of W354, indicating a predominance of the closed WpD loop conformer. The tryptophan fluorescence anisotropy decay measurements of the ligand-bound, wild-type *Yersinia* PTPase and of both ligation states of the C403S PTPase reveal a single correlation time of 30−48 ns due to the rotational motion of the protein, while the ligand-free, wild-type PTPase is found to have two correlation times of 31 and 3.8 ns. The 3.8 ns correlation time of the ligand-free enzyme is attributed to the hinged movement of the WpD loop which contains W354. These results indicate that under physiological conditions, the nonligated, wild-type *Yersinia* PTPase alternates between an open WpD loop and a closed loop form with a rate constant of $\sim 2.6 \times 10^8$ s^{-1}. We conclude that the rate of WpD loop closure of the wild-type *Yersinia* PTPase is thus independent of the presence of ligand, whereas in the presence of ligand the rate of opening is dramatically reduced resulting in a closed conformation on ligand binding. In contrast, the ligand-free and ligated C403S PTPase remain in the loop closed configuration over the time course of our dynamic measurements. The lack of WpD loop motion in the C403S PTPase is believed to be due to either a loss of repulsive potential between the anionic thiolate and Asp 356 of the WpD loop and/or the formation of a hydrogen bond or water bridged hydrogen bond between Ser 403 and Asp 356.

Many enzymes are characterized by fluctuating conformations which are coupled to the binding and release of substrate. For some enzymes, including triosephosphate isomerase, dihydrofolate reductase, and protein tyrosine phosphatases (PTPases),[1] the conformational change is restricted to the movement of a flexible loop that can be described as a hinged loop movement. For such enzymes it has been found that upon substrate binding, the loop folds over the active site−substrate complex to promote catalysis. Such motion may function to exclude solvent, recruit participating amino acids for catalysis or to stabilize and/or prevent loss of reactive intermediates. Crystallographic studies of loop open and closed structures have described the extent of the loop motion in various enzymes and have shown that movements as large as 11 Å are not uncommon (Bolin et al., 1982; Bystroff & Kraut, 1991; Bystroff et al., 1990; Lolis & Petsko, 1990; Wierenga et al., 1992; Stuckey et al., 1994). Yet in the majority of cases, the range and frequency of flexible loop motions remain undetermined (Gerstein et al., 1994). The relationship between microscopic protein dynamics and the rate of enzymatic catalysis remains unclear. Of central importance to understanding this relationship is whether the rate of loop closure is increased or decreased by ligand binding.

The protein tyrosine phosphatases, in combination with protein tyrosine kinases, regulate many intracellular signal transduction pathways. The PTPases catalyze the specific hydrolysis of the phosphate moiety of phosphotyrosine residues. The *Yersinia* PTPase was identified in the genus of bacteria responsible for the bubonic plague or "Black Death" (Guan & Dixon, 1990). Prokaryotic *Yersinia* PTPase and human PTPases share a common tertiary structure of their catalytic core as well as essential residues in the ligand binding site (Stuckey et al., 1994; Barford et al., 1994). The binding pocket is primarily composed of the phosphate binding loop or "P-loop" with the consensus sequence HCxxGxGR(S/T), which includes the nucleophilic cysteine (Guan & Dixon, 1991; Zhang et al., 1994a). The second component of the active site is an adjacent flexible binding loop, whose sequence is quite divergent except for the WpD sequence that includes the catalytic aspartic acid residue and a tryptophan residue near the hinge position of the loop

† Supported in part by a grant from the W. M. Keck Foundation to D. D. E. and by a National Institute of Health grant CA69202 to Z.-Y. Z.

* Author to whom correspondence should be addressed.

‡ Department of Physiology and Biophysics.

§ Department of Molecular Pharmacology.

⊗ Abstract published in *Advance ACS Abstracts,* February 1, 1997.

[1] Abbreviations: PTPase, protein tyrosine phosphatase; NMR, nuclear magnetic resonance; UVRR, ultraviolet resonance Raman; CW, continuous wave; UV ultraviolet; BBO, β-barium borate; CCD, charge-coupled detector; FWHM, full-width half-maximum.

S0006-2960(96)02213-1 CCC: $14.00

(Zhang et al., 1994b; Schubert et al., 1995). The flexible binding loop will hereafter be called the WpD loop (Schubert et al., 1995).

Several tetrahedral oxyanions, *e.g.*, arsenate, sulfate, and tungstate, act as competitive inhibitors for the *Yersinia* PTPase. The crystal structures for both ligand-free and tungstate-bound wild-type *Yersinia* PTPase have been determined (Stuckey et al., 1994). The crystal structure of an inactive variant of *Yersinia* PTPase complexed with sulfate has also been determined (Schubert et al., 1995) in which the essential nucleophilic cysteine 403 is mutated to serine. A comparison of these crystal structures shows that the WpD loop moves up to 6 Å between the ligand-free and the ligand-bound states (Stuckey et al., 1994; Schubert et al., 1995). *Yersinia* PTPase fortuitously contains only one tryptophan residue, W354, at one of the WpD loop hinges which is invariant among all the PTPases (Zhang et al., 1994b). The X-ray crystal structures suggest that the WpD loop of the *Yersinia* PTPase has two distinct conformations. In the "closed" state, Asp 356 on the WpD loop hydrogen bonds to the ligand, while in the "open" state, interactions between the WpD loop and the binding site are negligible (Stuckey et al., 1994). The loop conformation of the sulfate bound C403S mutant PTPase is similar to that of the ligand-bound native *Yersinia* PTPase, as revealed by its crystal structure (Schubert et al., 1995). The crystal structures of ligand-free and ligand-bound forms of human PTP1B and *Yersinia* PTPases have also revealed that in order for the loop to close about the oxyanion, a peptide bond in a β-turn must change its conformation significantly. Recently, Saper and co-workers (Schubert et al., 1995) have postulated that the wide range of catalytic rates observed in the PTPases may be due to the dynamics of the loop motion and that these dynamics may be partially determined by the third residue of the β-turn within the WpD loop.

The development of subnanosecond lasers and multidimensional NMR techniques over the past 20 years has allowed for the detailed characterization of protein dynamics. These techniques can be applied to the problem of the relationship between flexible binding loop motion and the rate-limiting step of enzymatic reactions. The recent NMR results of dihydrofolate reductase indicate that loop motions are associated with enzyme catalytic properties (Epstein et al. 1995). However, Williams and McDermott (1995) found in their solid-state NMR studies that the loop motion of triosephosphate isomerase was independent of ligation state.

We have examined the WpD loop motion of both the native and C403S mutant *Yersinia* PTPases by UVRR spectroscopy and time-resolved fluorescence measurements. The UVRR data indicate that the ligand-free native enzyme has almost equal populations of the loop closed and loop open conformers, whereas the ligated native enzyme exists in predominantly the loop closed conformation. The UVRR data for both forms of the C403S enzyme show the WpD loop to be overwhelmingly in the closed conformation. Time-resolved fluorescence anisotropy decay measurements show that the ligand-free native enzyme alternates between the two states with a time constant of $\sim(3.8\ \text{ns})^{-1}$. In contrast, neither the ligated native enzyme nor the ligation states of the C403S PTPase undergo significant dynamics on the nanosecond time scale.

MATERIALS AND METHODS

Enzyme Preparation. Yop51*/Δ162, an active variant of the native *Yersinia* PTPase, contains a C235R point mutation and lacks 162 amino acids at the NH_2 terminus (Zhang et al., 1992). Yop51*/Δ162 is kinetically indistinguishable from the full-length native enzyme and is the form used in the crystal structure studies. We shall refer to Yop51*/Δ162 as wild-type *Yersinia* PTPase in this paper. Homogeneous recombinant *Yersinia* PTPase was expressed and purified as previously described (Zhang et al., 1992). Aliquots of concentrated PTPase were diluted with 100 mM acetate buffer, pH 6.6, to obtain an optical density (1 cm path length) of 7−10 at the excitation wavelength (220−230 nm) corresponding to an enzyme concentration of approximately 50 μM. The concentration of the arsenate ligand was 17 mM, resulting in >90% of the enzyme in the ligated state (K_d of arsenate is 0.9 mM, Zhang et al., 1994a). The >90% arsenate-bound wild-type PTPase was used in both the UVRR and fluorescence decay experiments. The optical density was adjusted to ∼0.03 (1.8 μM) at the excitation wavelength of 300 nm and 1 cm path length for the fluorescence lifetime and anisotropy decay experiments. Laser-induced denaturation was monitored by comparison of absorption spectra taken before and after UV exposure and was found to be negligible.

Site-directed mutagenesis of residue Cys 403 of the *Yersinia* PTPase to Ser was carried out using the Muta-Gene *in vitro* mutagenesis kit from Bio-Rad (Zhang & Wu, 1997). The expression and preparation of homogeneous recombinant C403S mutant PTPase were performed as described (Zhang & Wu, 1997). Experimental conditions for the C403S mutant PTPase were identical with those used for the wild-type PTPase as described above.

UVRR Spectroscopy. A UVRR spectrometer was constructed using a continuous wave (CW), tunable UV laser source to avoid the saturation phenomena associated with pulsed sources (Asher et al., 1986; Ludwig and Asher, 1988). An argon ion laser (Coherent, Palo Alto, CA) operating in the multiline UV mode pumps an intracavity frequency-doubled ring dye laser (Coherent, Palo Alto, CA) with Stilbene 420 (Exciton, Inc., Dayton, OH) in ethylene glycol as the gain medium. The ring laser operates in a unidirectional mode with a single thin etalon. A 1 cm BBO doubling crystal allows for a tuning range of 218−232 nm with a maximum power of 6 mW at 226 nm. The typical UV power at the sample was 1 mW.

The UV excitation is focused onto a 1 cm square, quartz cuvette containing the protein solution. The lab-built cuvette holder provides for chilling to ∼4 °C and continuous stirring of the sample, as well as translation of the cuvette perpendicular to the optical axis for minimization of photoinduced denaturation. A stream of nitrogen gas across the cuvette face prevents water condensation.

The Raman signal was collected with a fused Suprasil triplet lens (CVI Laser Corp., Albuquerque, NM), focused with an f-matching lens onto the entrance slit of a 1.5 m single spectrograph (Sopra, Inc., Bois-Colombes, France) and passed through a polarization scrambler (Karl-Lambrecht, Chicago, IL). The spectrograph was equipped with a 3600 groove/mm holographic grating and a liquid nitrogen-cooled CCD detector (Princeton Instruments, Princeton, NJ). The spectrographic slit width was typically 180 μm giving <1

cm^{-1} resolution. The Raman signal was collected at 5 min intervals for a period of 30 min. The data were calibrated against the Raman spectra of cyclohexane, toluene, and 1,4-dioxane. All data processing, including the removal of artifactual cosmic ray peaks, was accomplished with the program SpectraCalc (Galactic Industries Corp., Salem NH). All spectral curve fits were modeled with 70% Lorentzian, 30% Gaussian functions. Sodium cacodylate was added as an internal standard (0.13 M final concentration, pH 6.6). The cacodylate Raman peak appears at 1280 cm^{-1}.

Time-Resolved Fluorescence and Anisotropy Decay. The time-correlated single-photon counting apparatus, based on the system of Chang *et al.* (1985) and optimized according to Holtom (1990), has been previously described (Gottfried et al., 1996). The instrument response function is typically 35 ps FWHM. Fluorescence anisotropy decay measurements were obtained using a sheet polarizer (Oriel 27340, Oriel Corp., Stratford, CT). The excitation and emission wavelengths were 300 and 350 nm, respectively, and the spectral band width was 16 nm for both the fluorescence lifetime measurements and the anisotropy decay measurements.

Fluorescence Anisotropy Data Analysis. The theoretical basis for our analysis has been previously described (Lakowicz, 1984), and only the most salient points are presented here for later reference. For a randomly oriented set of chromophores, plane polarized light excites a subset of the chromophores whose optical dipole is parallel to the incident light. In a Cartesian coordinate system, the decay of fluorescence intensity, $I(t)$ following the excitation pulse is given by

$$I(t) = I_{\parallel}(t) + 2I_{\perp}(t) \tag{1}$$

where $I_{\parallel}(t)$ is the time-dependent fluorescence parallel to the exciting light and $I_{\perp}(t)$ is the time-dependent fluorescence perpendicular to this plane.

The fluorescence anisotropy decay, $r(t)$, is defined as

$$r(t) = \frac{I_{\parallel}(t) - I_{\perp}(t)}{I(t)} \tag{2}$$

The decay of the anisotropy depends upon the excited state and molecular dynamics of the fluorophore. In the case of colinear absorption and emission dipole moments, the linear dependence of the anisotropy, $r(t)$, on the average value, $\langle \cos^2 \theta \rangle$ (where θ is the angle of the emission dipole relative to the plane of the polarized light), yields a maximum value of 0.4 for $r(t)$ (Lakowicz, 1984).

Furthermore, both the fluorescence and anisotropy decays can be described by a sum of exponentials:

$$I(t) = \sum_i A_i e^{-t/\tau_i} \tag{3}$$

$$r(t) = \sum_i r_i e^{-t/\phi_i} \tag{4}$$

where A_i and r_i are the normalized preexponential initial fluorescence intensities and initial anisotropies, respectively, and τ_i and ϕ_i are the corresponding fluorescence lifetimes and rotational correlation times. Equations 3 and 4 were used to obtain curve fits for the experimentally obtained fluorescence lifetime decay measurements and anisotropy decays using the Marquardt, nonlinear least-squares method. Determination of the quality of fit is judged from the value of the reduced χ^2, the runs test, the residuals, and the autocorrelation of the residuals (Grinvald & Steinberg, 1974). Estimation of error in the fitting parameters is done using the support plane method (χ^2 surface) (Johnson & Frasier, 1985).

For a chromophore which is rigidly attached to a spherical macromolecule, the rotational correlation time of the macromolecule, ϕ, may be calculated according to the Debye−Stokes−Einstein equation:

$$\phi = \frac{M\eta}{k_B T}(v + h) \tag{5}$$

where M is the macromolecular mass, η is the viscosity of the solvent, v is the specific volume of the protein, T is the absolute temperature, k_B is the Boltzmann constant, and h is the degree of hydration.

Internal motions that cause local movement of the chromophore can contribute additional terms to the anisotropy decay. These shorter correlation times can be qualitatively associated with local domain motions, but quantitation of the range of motion may be hampered by several factors (Szabo, 1984). This is especially true for tryptophan because excitation involves both the L_a and L_b dipole moments; subsequent rapid internal conversion between them adds a nonrotational contribution to the fluorescence anisotropy decay (Hansen et al., 1992; Ruggiero et al., 1990).

RESULTS

UVRR Spectroscopy. Raman spectra of proteins obtained with excitation between 220 and 230 nm results primarily in enhancement of the tryptophan and tyrosine vibrational modes (Fodor et al., 1989). The UVRR spectra of both ligand-free and arsenate-ligated wild-type and the C403S variant *Yersinia* PTPase obtained with 225 nm excitation are shown in Figure 1a and b, respectively. The Raman shift of the tryptophan and tyrosine bands as well as that of the internal cacodylate standard are given in Figure 1a and b. Additionally, bands not denoted in the figure include a broad band at ca. 1415 cm^{-1} with contributions from acetate and cacodylate and weak arsenate bands at 1405 and 1450 cm^{-1} in the arsenate ligated data. Similar spectra were obtained at excitation wavelengths of 220, 222, 228, and 230 nm. The Y8a and Y9a UVRR band positions for both C403S *Yersinia* PTPase states at 225 nm excitation and for both wild-type *Yersinia* PTPase states at 220, 225, and 230 nm excitation are given in Table 1. Additionally, the W3 curvefit peaks, along with the normalized peak areas, are listed in Table 1 for each *Yersinia* PTPase species.

The tryptophan Raman bands (arising from the single tryptophan, W354) which were found to differ between the ligand-free and ligated wild-type PTPase are the W3, W5, and W7 (Fermi doublet) bands (Figure 1a). The W3 band is especially noteworthy because it is expected to be a single peak in a protein containing one tryptophan residue. As demonstrated in the curvefitting results of Figure 2, the W3 band of wild-type nonligated *Yersinia* PTPase (Figure 2a) is essentially a doublet of approximately equal intensity bands at 1549 and 1559 cm^{-1} with a much weaker band at 1544 cm^{-1}. Repeated curvefits to the W3 band of the nonligated wild-type PTPase showed that the ratio of the sum of the area of the 1544 and 1549 cm^{-1} bands to the area of the

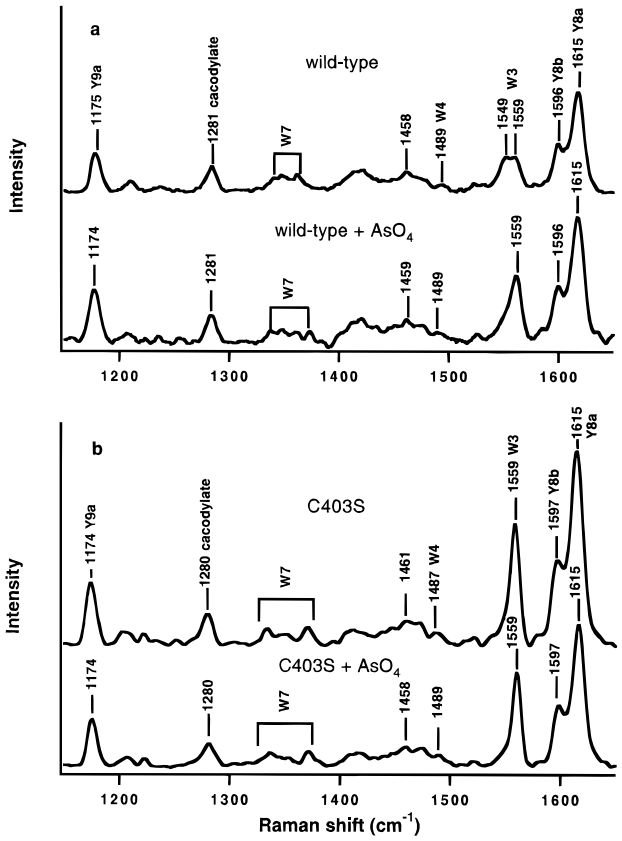

FIGURE 1: (a) Ultraviolet resonance Raman spectra of wild-type *Yersinia* PTPase in 100 mM acetate buffer, pH 6.6, 10 °C, 225 nm excitation. Top: ligand-free PTPase. Bottom: arsenate-ligated PTPase. (b) Ultraviolet resonance Raman spectra of mutant C403S *Yersinia* PTPase in 100 mM acetate buffer, pH 6.6, 10 °C, 225 nm excitation. Top: ligand-free mutant PTPase. Bottom: arsenate-ligated mutant PTPase.

1559 cm^{-1} band was constant (data not shown). We note further that the absolute peak frequency of the primary bands varied by no more than ± 1 cm^{-1} (Table 1). In the presence of ligand, the W3 band of the wild-type enzyme is dominated by the 1559 cm^{-1} peak (Figure 2b and Table 1). In addition, the complex Fermi doublet is found to be a composite of three to four bands (1336, 1346, 1359, and 1371 cm^{-1}) that vary in relative intensity between the ligand free and ligated complexes (Figure 3a and b).

The UVRR spectra of the mutant C403S PTPase for the two ligation states are nearly identical (Figure 1b). The W3 bands of both states of the C403S mutant PTPase are dominated by the 1559 cm^{-1} peak which is the same W3 position observed in the ligated wild-type spectrum (Figure 2c and d). Differences in the other primary UVRR bands were found to be similar to those observed between the two ligation states of the wild-type PTPase (Figure 1b and 3c and d). The W7 bands of the two ligation states of C403S PTPase are shown in Figure 3c and d. The primary difference between the W7 bands is the shift of the 1346 cm^{-1} band to 1343 cm^{-1} upon ligand binding (Figure 3c and d). In addition, there are small intensity changes in the four W7 bands. The ca. 1460 cm^{-1} band was found to shift down 3 cm^{-1} upon ligand binding and likely has contributions from both the W5 vibration and the proline imide II vibration.

Fluorescence Intensity and Anisotropy Decays. The fluorescence decay data of ligand-free and arsenate-bound wild-type *Yersinia* PTPase were each fit to a sum of three exponential components (eq 3). These results are summarized in Table 2. For both ligation states of the wild-type enzyme, the lifetimes are similar in value: 1, 3, and 7 ns. The amplitudes (A_i) are roughly equal for the nonligated wild-type enzyme whereas the amplitude for the longest lifetime increases at the expense of the shortest lifetime for the arsenate-ligated wild-type enzyme. The result is a longer average lifetime for the arsenate-ligated wild-type enzyme. In the case of the nonligated C403S mutant PTPase, only two lifetimes are obtained, 2.61 and 7.91 ns, with an amplitude ratio of approximately 1:9 resulting in an average lifetime of 6.67 ns. The fluorescence lifetime of the arsenate-ligated mutant PTPase was found to be well-described by a single lifetime of 7.9 ns.

The fluorescence anisotropy decays for the ligand-free and arsenate-ligated wild-type and C403S mutant PTPases are shown in Figure 4a and b, respectively. The results of the curvefits to the wild-type and C403S mutant PTPase anisotropy decays are summarized in Table 3. The anisotropy decay of the ligand-free wild-type PTPase (Table 3) was best fit to a sum of two exponentials (eq 4) with correlation times (ϕ_i) of 3.8 and 31 ns and corresponding initial anisotropies (r_i) of 0.04 and 0.24. The anisotropy decay of the arsenate-ligated wild-type enzyme (Table 3) was described equally well by either single exponential or two exponential fits. On the basis of one standard deviation confidence interval and the wide variance in the short correlation time of different double exponential fits, we emphasize that the arsenate ligated wild-type enzyme should be considered as a single exponential with a correlation time of 42 ns and an initial anisotropy of 0.28. The fits to the anisotropy decays of both ligation states of the C403S mutant PTPase yielded single

Table 1: UVRR Band Positions for Both Binding States of Wild-type and C403S *Yersinia* PTPase over the Excitation Range 220−230 nm. For the Y8a and Y9a Bands, the Single Peak Maxima Are Given; for the W3 Band, the Curvefit Peaks are Listed, with the Normalized Peak Area in parentheses

excitation wavelength (nm)	W3	Y8a	Y9a
	nonligated WT		
220	1548 (0.50) 1558 (0.50)	1616	1176
225	1544 (0.08) 1549 (0.43) 1559 (0.49)	1615	1174
230	1547 (0.18) 1550 (0.33) 1560 (0.49)	1617	1176
	arsenate-ligated WT		
220	1544 (0.094) 1549 (0.18) 1559 (0.73)	1615	1176
225	1544 (0.06) 1549 (0.18) 1559 (0.75)	1615	1174
230	1549 (0.21) 1560 (0.79)	1617	1175
	nonligated C403S		
225	1549 (0.067) 1559 (0.93)	1615	1174
	arsenate-ligated C403S		
225	1549 (0.072) 1559 (0.93)	1616	1174

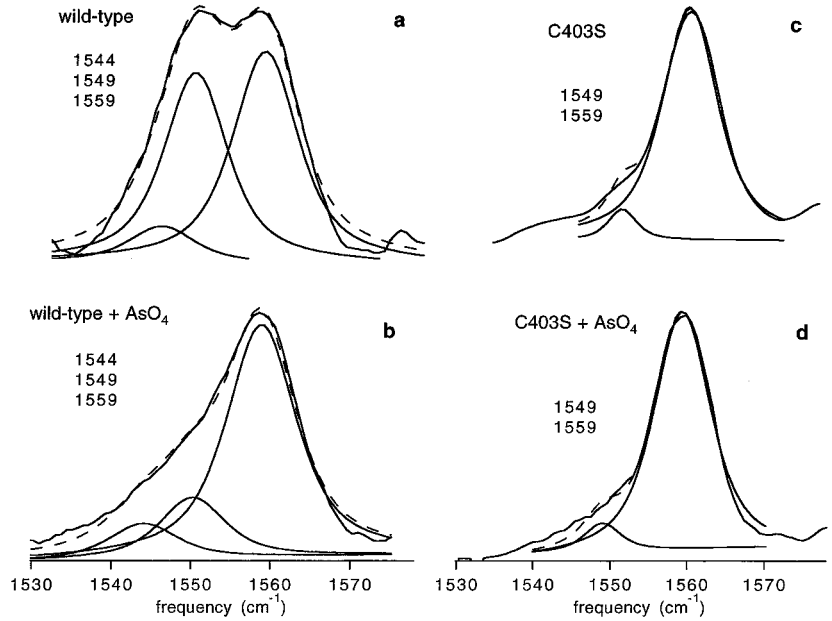

FIGURE 2: UVRR spectra of the W3 band (solid lines) and curve fits (dashed lines) for (a) the ligand-free wild-type *Yersinia* PTPase, (b) arsenate-ligated wild-type PTPase, (c) ligand-free C403S PTPase; and (d) arsenate-bound C403S PTPase. The peak positions of the W3 fit component curves are listed for each spectra.

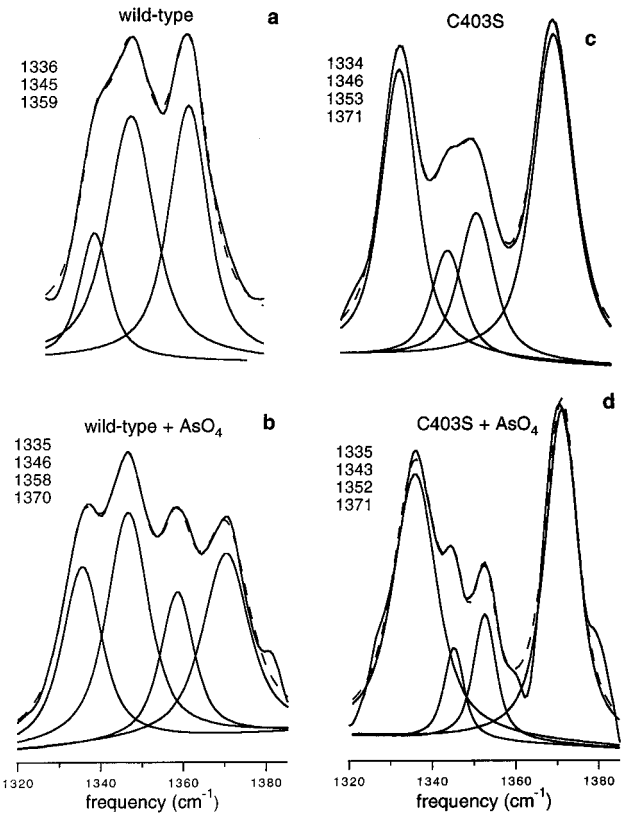

FIGURE 3: UVRR spectra of the W7 band (solid lines) and curve fits (dashed lines) for the ligand-free wild-type *Yersinia* PTPase (3a, top, left), arsenate-ligated wild-type PTPase (3b, bottom, left), ligand-free C403S PTPase (3c, top, right) and arsenate-bound C403S PTPase (3d, bottom, right). The peak positions of the fit component curves are listed for each spectra.

correlation times for both data sets. Once again, we note that double exponential fits of the data did not yield statistically significant improvements of the fits and that a wide variance in the optimized parameters for equivalent fits further indicated that a biexponential correlation time was not warranted. For the nonligated C403S mutant PTPase, the best fit yielded an initial anisotropy of 0.30 with a correlation time of 36 ns while the fit to the arsenate-ligated mutant PTPase data produced an initial anisotropy of 0.25 with a correlation time of 30 ns.

DISCUSSION

Tryptophan 354: W3 Vibration and Conformation. The crystal structures of the two *Yersinia* PTPase states indicate that upon ligand binding, the W354 $\chi^{2,1}$ torsion angle changes from an open loop rotamer of approximately $-71°$ to $-80°$ to a closed loop rotamer of $-4°$.[2] Although the W3 mode is due to a pyrrole ring stretching vibration, the frequency of the W3 vibration has been shown by Miura et al. (1989) to be a function of the $\chi^{2,1}$ dihedral angle (Figure 5). The W3 regions of the ligand-free and ligated wild-type and C403S mutant PTPase spectra are shown in Figure 2. The W3 band for the ligand-free wild-type enzyme is resolved into two peaks of similar intensity centered at 1549 and 1559 cm^{-1}, with a small third peak at 1544 cm^{-1}, indicating the presence of at least two tryptophan conformers. The ligated wild-type enzyme is dominated by the 1559 cm^{-1} band with minor contributions from the 1544 and 1549 cm^{-1} bands. The arsenate-bound wild-type PTPase was prepared such that 90% of the enzyme would be ligand-bound. The small 1544 and 1549 cm^{-1} peaks are attributed to a small amount of ligand-free enzyme which is partly in the open loop conformation. The 1559 cm^{-1} peak is associated with the ligand-bound state.

The X-ray structure of the C403S mutant PTPase crystal grown with sulfate shows that this inhibitor occupies the active site (Schubert et al. 1995). Presumably, arsenate in solution complexes with the C403S mutant PTPase in a similar fashion. The W3 bands for both the nonligated and arsenate-ligated C403S mutant PTPase are resolved into a dominant peak at 1559 cm^{-1} and a very small peak at 1549 cm^{-1} (Figure 2c and d). The fractional percent of the 1549

[2] Two different ligand-free structures have been solved by Saper and co-workers which show slight differences in the $\chi^{2,1}$ angle, $-71°$ (Stuckey et al., 1994) and $-80°$ (Schubert et al., 1995).

Table 2: Fluorescence Decay Amplitudes (A_i), Lifetimes (τ_i, ns), Average Lifetimes ($\langle\tau\rangle$, ns), and Quality of fit (χ_r^2) for *Yersinia* Nonligated and Arsenate-Ligated Wild-type (WT) and C403S (Mutant) PTPase. One Standard Deviation Confidence Intervals Are Shown in Parentheses. The Excitation Wavelength was 300 nm, Emission Wavelength, 350 nm, and Spectral Band Width, 16 nm

	A_1	τ_1	A_2	τ_2	A_3	τ_3	$\langle\tau\rangle$	χ_r^2
nonligated WT	0.383 (0.335−0.430)	0.713 (0.580−0.850)	0.337 (0.304−0.370)	2.82 (2.45−3.30)	0.278 (0.250−0.302)	7.35 (7.18−7.60)	3.28	1.12
arsenate-ligated WT	0.132 (0.0885−0.200)	0.781 (0.446−1.30)	0.348 (0.304−0.382)	3.15 (2.66−3.98)	0.520 (0.433−0.560)	6.98 (6.84−7.22)	4.83	1.13
nonligated C403S			0.102 (0.099−0.177)	2.61 (2.08−4.60)	0.898 (0.791−0.997)	7.91 (7.86−8.17)	6.67	1.06
arsenate-ligated C403S					1.0	7.85 (7.78−7.86)	7.85	1.26

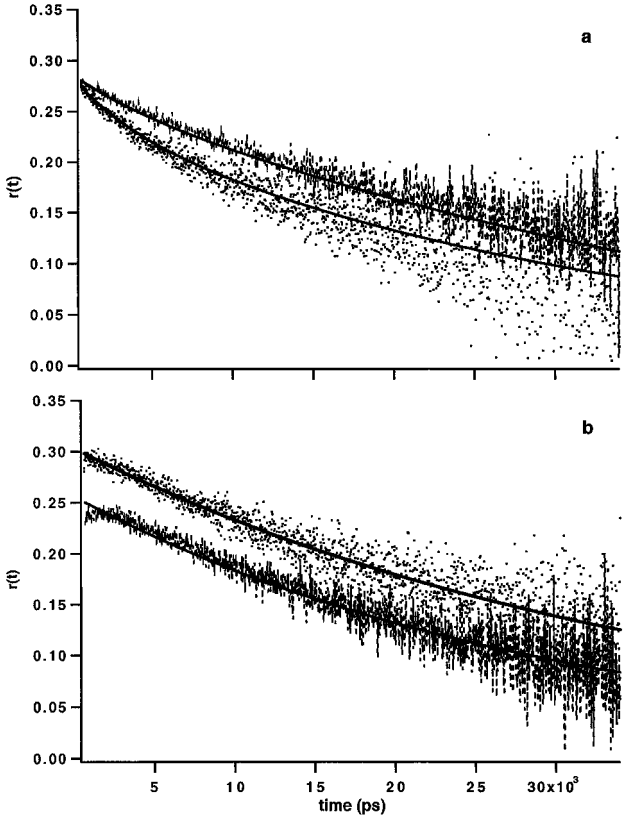

FIGURE 4: Fluorescence anisotropy decays of *Yersinia* PTPase in 100 mM acetate buffer, pH 6.6, 10 °C, 300 nm excitation, 350 nm emission, 16 nm spectral band width. The solid lines through the data are the fits to eq 4. (a) Dot: ligand-free wild-type PTPase. Dashed line: arsenate-ligated wild-type PTPase. (b) Dot: ligand-free C403S mutant PTPase. Dashed line: arsenate-ligated C403S mutant PTPase.

Table 3: Best Fits to the Anisotropy Decays, Quality of Fit (χ_r^2) and Limits of the Anisotropy Analysis for the Wild-type (WT) and C403S *Yersinia* PTPase Showing the Range of Parameter Values (ϕ_1, ϕ_2, Correlation Times; r_1, r_2, Initial Anisotropies) Near One Standard Deviation Confidence Intervals

	ϕ_1 (ns)	r_1	ϕ_2 (ns)	r_2	χ_r^2
nonligated WT	3.82	0.040	30.6	0.24	1.39
	1.80	0.031	26.8	0.25	1.43
	5.50	0.040	34.7	0.23	1.43
arsenate-ligated WT	4.00	0.016	48.2	0.26	1.91
		0.0	42.2	0.28	1.97
	8.0	0.012	46.9	0.26	1.95
nonligated C403S		0.0	36.2	0.30	1.39
		0.0	35.0	0.30	1.42
		0.0	38.0	0.29	1.42
arsenate- ligated C403S		0.0	29.7	0.25	1.48
		0.0	27.9	0.26	1.54
	9.20	0.02	33.0	0.24	1.50

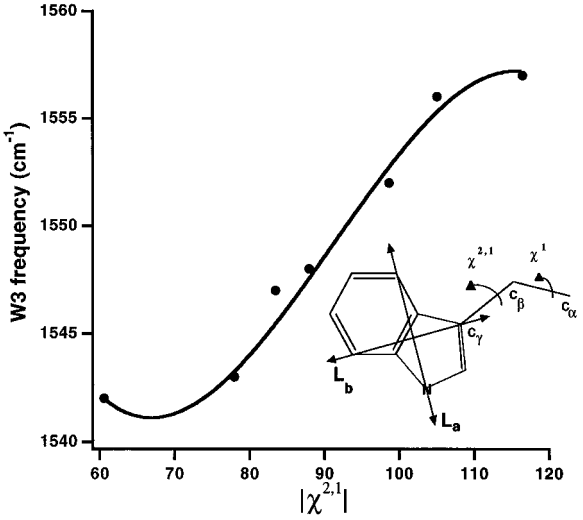

FIGURE 5: UVRR W3 band frequency plotted as a function of the absolute value of the dihedral angle, $\chi^{2,1}$. The sigmoidal curve shows a fit with a third-order spline function. Reproduced by permission of John Wiley & Sons, Ltd, from Miura et al., (1989) *J. Raman Spectrosc. 20*, 667−671. Copyright (1989) John Wiley and Sons. Insert: tryptophan indole ring including the L_a and L_b dipole moments, the location of the C_α, C_β, and C_γ atoms, and the rotational direction for the dihedral angles, $\chi^{2,1}$ and χ^1.

cm^{-1} peak for the two mutant PTPase states are essentially equal (Table 1; 7% of W3 band), indicating that the presence of the arsenate ligand has little effect on the equilibrium of the two conformers.

The Miura et al. plot of $|\chi^{2,1}|$ versus W3 frequency (Figure 5) indicates that the low frequency 1544 and 1549 cm^{-1} bands correspond to $\chi^{2,1}$ dihedral angles of ±79° and ±90°, respectively. The high-frequency band at 1559 cm^{-1}, however, lies outside the frequency range of the Miura et al. data. The ligand-free wild-type enzyme X-ray crystal structures show that the W354 $\chi^{2,1}$ dihedral angle is approximately −71° to −80°, corresponding to a Raman frequency of 1542−1544 cm^{-1} (Figure 5). As Figure 2 illustrates, a $\chi^{2,1}$ rotamer with a corresponding W3 band at 1544 cm^{-1} only represents a small fraction of the equilibrium wild-type PTPase structures. The wild-type PTPase−WO_4^{-2} crystal structure indicates that the W354 $\chi^{2,1}$ dihedral angle is −4° in the ligated, closed loop state. Furthermore, the crystal structure of the sulfate-bound C403S mutant PTPase is superimposable on that of the tungstate-bound wild-type *Yersinia* PTPase (Schubert et al., 1995), indicating that the former species is also in a closed loop conformation. The −4° angle also lies outside the $\chi^{2,1}$ dihedral angle range of the Miura et al. plot. The curve fits to the W3 band of the

arsenate bound mutant PTPase yield essentially a single band at 1559 cm^{-1} (Figure 2b). The plot of Miura et al. does not extend to 1559 cm^{-1}, and thus we cannot assign a $\chi^{2,1}$ dihedral angle with certainty. However, it seems reasonable to cautiously assign this band to the $-4°$ rotamer, since the 1559 cm^{-1} peak is associated with the ligand-bound state.

A visual inspection of the steric environment of the W354 side chain (Insight, Biosym Inc., San Diego, CA) reveals that in the loop closed crystal structure there is very little possibility for W354 sidechain motion. The only reasonable Trp rotamer is the $\chi^{2,1} = -4°$ rotamer that is observed in the crystal structure (Stuckey et al., 1994). In the ligand-free wild-type PTPase, there is a slightly less crowded Trp environment. At least four possible Trp rotamers can exist at $\chi^{2,1} = -71°$, $-80°$, $-95°$, and $100°$ for which there are no large steric clashes with other atoms. As discussed above, our Raman data indicates that a $-71°$ to $-80°$ rotamer (corresponding to a W3 position of 1542−1544 cm^{-1}) is a small fraction of the solution equilibrium structures. Rotamers at $\chi^{2,1} = -95°$ and $100°$ would correspond to W3 bands at 1551 and 1553 cm^{-1}, respectively. Our data do not show evidence for bands at these positions; rather we observe a band at 1549 cm^{-1} corresponding to a $\chi^{2,1} = -90°$. Thus, our Raman data indicates that the ligand-free wild-type enzyme exists in both open and closed loop conformations, $\chi^{2,1}$ of $-90°$ and $-4°$, while both the ligated native PTPase and both ligation states of the C403S mutant PTPase are in a closed loop conformation, $\chi^{2,1} = -4°$.

Tryptophan 354: Fermi Doublet. The W7 Raman band is a doublet resulting from a Fermi resonance interaction of the W7 band (1340 cm^{-1}) with a combination band consisting of two vibrations of 930 and 423 cm^{-1} (Harada et al., 1986; Takeuchi & Harada, 1986). The result of this interaction is usually a doublet with peaks at approximately 1340 and 1360 cm^{-1} whose intensity ratio varies with the amount of water present in the indole ring environment (Miura et al., 1988; Jordan et al., 1995). The native and C403S PTPase W7 bands are unusually complex consisting of not less than three peaks (1336, 1346, and 1359 cm^{-1}) of varying intensities (Figure 3). Excitation at four additional wavelengths from 220 to 230 nm similarly yielded complex W7 bands for both wild-type enzyme states (data not shown). In addition, the ligated wild-type and mutant PTPase spectra contain a fourth band at ca. 1370 cm^{-1} of significant intensity. In each of the five UVRR spectra of the ligand-free wild-type PTPase obtained at different excitation wavelengths, the 1359 cm^{-1} peak was of greater intensity than either the 1336 or 1346 cm^{-1} peaks (Figure 3a and b, additional data not shown). In contrast, the ligated wild-type enzyme UVRR spectra show the 1359 cm^{-1} band to be slightly weaker than the 1336 or 1346 cm^{-1} bands. For excitation at 225 nm, the W7 bands for both states of the C403S mutant PTPase were similar to those of the arsenate-ligated wild-type PTPase in that the 1334−1335 cm^{-1} peak is larger than the 1336 cm^{-1} peak of the nonligated wild-type enzyme and a large peak at 1371 cm^{-1} is present (Figure 3). We do not have an explanation for the origin of the 1370 cm^{-1} peak but believe it to be associated with the loop closed conformation. The shift of the 1346 cm^{-1} component to 1343 cm^{-1} in the presence of arsenate provides an independent verification that the ligand indeed binds to the C403S enzyme. Finally, the C403S PTPase W7 band at 1353 cm^{-1} is shifted 6 cm^{-1} to lower energy relative to the wild-type enzyme W7 peak at 1359 cm^{-1}.

A strong 1359 cm^{-1} band has been associated with a nonaqueous tryptophan environment in both nonresonant Raman and UVRR spectroscopy (Harada et al., 1986; Jordan et al., 1995). The UVRR results for the ligand-free wild-type enzyme indicate that the environment of W354 is nonaqueous. The crystal structure also depicts the W354 indole ring tightly enveloped by nearby residues. The computed solvent-exposed surface area for W354 (Richmond, 1984) is <3% of the total surface area of tryptophan for both loop open and loop closed crystal forms of the wild-type enzyme. Thus, both ligand-free loop conformations of *Yersinia* PTPase are characterized by an indole ring within a nonaqueous environment.

The W7 data for the ligated wild-type enzyme and both forms of the mutant enzyme are more difficult to interpret due to the appearance of a fourth component at 1371 cm^{-1}. A conventional interpretation of the UVRR data would be that the indole ring is in an aqueous environment. Yet the crystal structure and the fluorescence emission maximum of the ligand-bound wild-type PTPase of 338 nm (Zhang &Wu, 1997) each strongly argue that the indole ring is in a nonaqueous environment. In addition, in other UVRR studies we have found similar tryptophan Fermi enhancement patterns that included a 1370 cm^{-1} band (Juszczak & Eads, unpublished data). Therefore, we conclude that the indole ring is in a nonaqueous environment and that the closed loop conformation exhibits an anomalous Fermi resonance interaction of the fundamental mode and the combination modes.

Fluorescence Lifetime Measurements. The utility of the tryptophan fluorescence decay as an indicator of protein dynamics is problematic as many proteins that contain a single tryptophan exhibit nonexponential decays (Beechem & Brand, 1985; James et al., 1985; Chen et al., 1987; Gryszynski et al., 1988; Chen et al., 1991). Due to the complexity of the tryptophan fluorescence decay, quantitative assignments of decay components to individual conformational states is essentially impossible in the absence of supporting data. The fluorescence lifetimes and corresponding amplitudes of ligand-free and ligated wild-type *Yersinia* PTPase and C403S mutant *Yersinia* PTPase are given in Table 2. The minimum number of decay components necessary to describe the wild-type PTPase fluorescence decay is 3 exponentials. Multiple fluorescence lifetimes of single tryptophan proteins have been ascribed to multiple Trp rotamer conformations (Chen et al., 1991; Szabo & Rayner, 1980), to multiple quenching pathways, to multiple energy transfer pathways (Bajzer & Prendergast, 1993), and/or to solvent relaxation. Since the W354 UVRR data and crystal structure indicate that the equilibrium population of the arsenate-bound wild-type PTPase is dominated by one rotamer conformation, assignment of the three lifetimes to individual W354 rotamers is unreasonable. Greater differences are found in the corresponding amplitudes. While the amplitudes are nearly equal for the ligand-free wild-type PTPase (Table 2), the amplitude of the longest lifetime of the arsenate-bound wild-type PTPase almost doubles at the expense of the amplitude of the shortest lifetime. The amplitudes of the intermediate lifetime are similar for both enzyme forms. Thus, the shortest lifetime of ∼0.74 ns is associated with the loop open PTPase form while the longest

lifetime of ~7.0−7.4 ns dominates the decay processes of the closed loop form of the enzyme.

The W354 UVRR data of the ligand-free and ligand-bound C403S mutant PTPase point to a single conformation for W354. Fluorescence lifetime measurements yielded two significant lifetimes of 2.6 and 7.9 ns for the nonligated C403S PTPase and one lifetime of 7.9 ns for the arsenate-bound C403S PTPase. The amplitude of the 2.6 ns lifetime for nonligated C403S PTPase is only 10% of the total, resulting in an average lifetime of 6.7 ns, longer than the average lifetime for either form of the wild-type PTPase (Table 2). The monoexponential lifetime of 7.9 ns for the arsenate-ligated mutant PTPase is atypical of even single tryptophan-containing proteins. The lack of complex tryptophan photophysics indicates negligible solvation, which is consistent with the blue fluorescence emission maximum of 338 nm, no energy transfer or electron transfer and a single rotamer for the indole side chain with negligible dynamics. Thus, we conclude that the arsenate-ligated C403S PTPase WpD loop undergoes little dynamics on the nanosecond time scale.

Fluorescence Anisotropy Measurements and Loop Motion. Measurements of the correlation times of individual residues by either NMR spectroscopy or fluorescence anisotropy decay provides a means by which the dynamics of the protein can be probed. The long fluorescence anisotropy decay times or correlation times (ϕ_2) were obtained from fits of the raw data (Figure 4) to eq 4. These long correlation times of approximately 30−48 ns for both PTPase forms correspond to the rotational correlation time for the macromolecule. The hydrodynamic rotational correlation time for both enzymes as calculated from the Debye−Stokes−Einstein equation (eq 5) is 22 ns (h = 0.2 g of water/g of protein). The lower value of the calculated rotational correlation time may be attributed to the nonspherical shape of the protein and/or a larger effective solvation shell (Lakowicz, 1984). Generally, experimental values of the rotational correlation time are roughly twice that expected for an anhydrous sphere (Yguerabide et al., 1970). The spread in values obtained experimentally for the rotational correlation time is due to the fact that the average fluorescence lifetime is almost an order of magnitude less than the long correlation time of the anisotropy decay. Thus, the fluorescence signal level is weak at 20−100 ns where the data is critical for accurately determining the value of the rotational correlation time.

The most intriguing result of the fluorescence anisotropy experiment is the additional 3.8 ns decay of the ligand-free wild-type enzyme. In principle, the two correlation times obtained for the ligand-free enzyme could be attributed to a change in the overall protein shape, rather than to a localized conformational change. If the molecular shape is ellipsoidal rather than spherical, two rotational correlation times would be expected for the ligand-free enzyme: one for rotation around the ellipsoidal axis, and another for rotation perpendicular to that axis (Szabo, 1984). This possibility can be ruled out, since the crystal structures of the ligand-bound and ligand-free PTPase are superimposable with the exception of the WpD loop (Stuckey et al., 1994; Schubert et al., 1995) and only one significant correlation time is observed for the bound form. In addition, the shortest correlation time for a rigid prolate ellipsoid cannot be less than 95% of the rotational correlation time calculated from the Debye−Stokes−Einstein equation (Tao, 1969). We thus attribute the 3.8 ns correlation time of the ligand-free PTPase to a localized motion of the tryptophan and/or the WpD loop.

The two possible motions of W354 are rotations about the C_α−C_β and C_β−C_γ bonds (Figure 5), which could be either independent of or a result of the loop motion. If the W354 motion is independent of the loop motion, the anisotropy decays for both forms of the enzyme would be identical. Furthermore, unhindered motion of W354 implies an aqueous environment, but our UVRR W7 band results, the X-ray crystal structure (Stuckey et al., 1994), as well as the absorption and fluorescence spectra (Zhang et al., 1992) all point to a nonaqueous and sterically constrained environment for W354. We conclude that W354 in the ligand-free enzyme is characterized both by hindered motion and a nonaqueous environment.

Since local rotation of W354 is too limited to affect the anisotropy decay, it can be deduced that the motion of the entire WpD loop is responsible for the 3.8 ns correlation time of the ligand-free enzyme. The picture that emerges from the UVRR results for the ligand-free enzyme is an equilibrium structure of two W354 rotamers: a $\chi^{2,1} = -90°$ open WpD loop rotamer and a second rotamer that we have assigned as the $\chi^{2,1} = -4°$ closed WpD loop rotamer. These rotamers must also predict the fluorescence anisotropy decay. Assuming the L_a and L_b dipole moments are at right angles (Eftink et al., 1990), an indole ring rotation from the −4° rotamer position to the −90° position results in an angular change of 36° for the L_a dipole moment and a 20° change for the L_b dipole moment. The fast, 3.8 ns correlation time of the ligand-free PTPase is thus consistent with WpD loop motion between open and closed forms where the W354 $\chi^{2,1}$ angles are as predicted from the UVRR data. In contrast, if we consider the rotameric structures that are found in the crystal structures, *i.e.*, −4° and −71°, then the L_a dipole moment angular change is only 9° and that for the L_b dipole moment is 11°. This angular displacement of the transition dipole moments is quite small, and is expected to yield a single exponential anisotropy decay for the non-ligated wild-type enzyme, which is not observed.

We now consider the implication of these measurements on the motion of the ligand-free wild-type PTPase. The fluorescence anisotropy measurements indicate a nanosecond motion that is attributable to the movement of the WpD loop between the open and closed conformation. This movement is coupled to a rotation of the W354 indole side chain. Furthermore, our Raman data indicate that the equilibrium population of the two rotamers is approximately equal. Consistency of these two measurements requires that the rate of loop closing (k_1) is approximately equal to the rate of loop opening (k_{-1}):

$$E_{\text{open}} \underset{k_{-1}}{\overset{k_1}{\rightleftharpoons}} E_{\text{closed}}$$

As the fluorescence anisotropy indicates, the rate of loop-induced indole motion is $(\sim 4\ \text{ns})^{-1}$, thus we can assign $k_1 \approx k_{-1} \approx 2.6 \times 10^8\ \text{s}^{-1}$. Due to the fact that this rate is near that of the free diffusion of such a loop segment, we also conclude that the energy barrier between the open and closed forms is very small.

In a similar manner we consider the ligand-bound PTPase measurements. The Raman data indicate that the equilibrium population is dominated by the rotamer corresponding to

1559 cm^{-1}, which we have assigned as the $\chi^{2,1}$ rotamer of $-4°$. The fluorescence anisotropy data indicates that there is little motion on the nanosecond time scale (Table 3). On the basis of these data and the crystal structure which shows that the WpD loop closes upon ligand binding, we can conclude that for the ligated enzyme $k_1 \gg k_{-1}$:

$$E \cdot L_{\text{open}} \underset{k_{-1}}{\overset{k_1}{\rightleftharpoons}} E \cdot L_{\text{closed}}$$

Furthermore, as the rate of loop motion of the ligand-free PTPase is on the order of one-dimensional diffusion of the segment, we do not believe that the origin of the difference between the relative rate constants arises from an increase in the rate of loop closing, but rather to a decrease in the rate of loop opening. In other words, the ligand stabilizes the closed loop conformation.

We now consider the C403S PTPase. The ligand-free and ligand-bound C403S PTPase fluorescence anisotropy decays are both well described by single correlation times that are on the order of the long rotational correlation times observed in the wild-type PTPase decays (Table 3). The lack of a short correlation time in the ligand-free C403S PTPase anisotropy decay indicates that the WpD loop does not move during the time course of these measurements. This is in stark contrast to the ligand-free wild-type PTPase which undergoes significant motion on a time scale of less than 10 ns.

We believe that this difference between wild-type and C403S loop dynamics can be explained in terms of the effect of the C403S mutation on the electrostatics of the binding pocket. As has been established, the C403 residue in *Yersinia* wild-type PTPase exists as the thiolate anion at our experimental pH of 6.5−6.6 as it has an apparent pK_a of 4.7 (Zhang & Dixon, 1993). This can be compared to the aqueous cysteine pK_a of 8.5, which indicates that the active site environment of the PTPase stabilizes the negative charge. While the pK_a of the S403 alcohol group in the mutant PTPase is unknown, serine's aqueous pK_a of 13.4 and the relative shift in the cysteine pK_a values lead us to the assumption that the serine alcohol does not exist as the oxy-anion in C403S PTPase at our experimental pH of 6.5−6.6. Thus, the effect of the mutation is not a simple substitution of an alcohol group for the thiol group, but rather a replacement of the charged thiolate with a neutral (albeit polar) alcohol. Another key point is that the carboxylate portion of the catalytic aspartic acid side chain of the WpD loop (D356) likely comes within a few angstroms of the C403S side chain in the closed loop conformation. The former residue is also anionic in character so neutralization of the binding site by the C403S mutation will lower the electrostatic repulsion between the binding pocket and the WpD loop. Furthermore, S403 has the potential to form a hydrogen bond to D356 either directly or through bridging water molecules. Each of these factors will favor the closed loop conformation in the C403S enzyme.

One possible result of the C403S PTPase mutation as discussed above is that the energy for the closed loop conformation is significantly lower than the open loop conformation. Thus, rather than oscillating between an open and closed form, with the concomitant change in the $\chi^{2,1}$ angle (Raman W3 mode) and dipole motion (fluorescence anisotropy), the C403S PTPase WpD loop remains predominately closed even in the absence of a ligand. Upon anionic ligand binding to the C403S PTPase, the WpD loop motion appears further reduced as evidenced by the long, single exponential tryptophan fluorescence lifetime obtained for the ligated mutant enzyme (Table 2).

Concluding Remarks. We have studied the WpD loop (residues 351−359) motion of wild-type and C403S mutant *Yersinia* PTPase under physiological conditions by steady-state UVRR spectroscopy and time-resolved fluorescence lifetime and fluorescence anisotropy measurements. The UVRR results show that the equilibrium population of W354 in the native ligand-free PTPase is almost equally split between two $\chi^{2,1}$ dihedral angles as represented by the 1549 and 1559 cm^{-1} W3 Raman bands. On the basis of the data of Miura et al. (1989) and the PTPase crystal structures (Stuckey et al., 1994; Schubert et al., 1995), we have assigned the 1549 and 1559 cm^{-1} W3 Raman bands to $\chi^{2,1}$ rotamer angles of $-90°$ and $-4°$, respectively. In contrast, the equilibrium population of W354 in the arsenate-bound wild-type PTPase and both the ligand-free and arsenate-ligated C403S PTPases is dominated by a single Trp 354 rotamer (1559 cm^{-1}) assigned to the $\chi^{2,1}$ dihedral angle of $-4°$. The $-4°$ $\chi^{2,1}$ rotamer conformation of Trp 354 is therefore associated with the closed WpD loop, and the $-90°$ rotamer dominates the open WpD loop state.

The time-resolved fluorescence lifetime measurements show that a long radiative lifetime of 7−8 ns is associated with the closed loop state of both native and C403S *Yersinia* PTPase and a shorter radiative lifetime of 0.7−0.8 ns with the open loop state. Fluorescence anisotropy decay measurements yield a 30−48 ns correlation time that corresponds to the rotational motion of the macromolecule. Significantly, the anisotropy decay of the ligand-free wild-type PTPase exhibits an additional 3.8 ns component which is coupled to the WpD loop motion.

The C403S PTPase fluorescence anisotropy decay measurements yield a single long rotational correlation time that is also due to the rotational motion of the macromolecule. The net effect of the C403S mutation is to replace the anionic thiolate with an uncharged polar OH group. This loss of charge lowers the energy of the closed WpD loop conformation such that the open WpD loop conformation in the C403S PTPase is undetectable under our fluorescence measurement conditions. Thus, a delicate balance between the electrostatics of the binding pocket and the WpD loop has evolved in the native *Yersinia* PTPase. The binding pocket must facilitate the binding of the substrate oxyanion tyrosine phosphate, without stabilizing the closed loop conformation in the unligated state where D356 of the WpD loop becomes a pseudoligand. On the basis of our UVRR spectroscopy results and time-resolved fluorescence lifetime and anisotropy decay measurements for both native and C403S PTPase, we conclude that the C403S PTPase WpD loop overwhelmingly adopts the closed conformation independent of the presence of a ligand due to the loss of the repulsive thiolate charge and/or the formation of a hydrogen bond between S403 and D356.

In summary, the catalytic WpD loop motion in wild-type *Yersinia* PTPase occurs continuously and rapidly in the absence of substrate with opening and closing rates that are approximately equal, resulting in a nearly equal distribution of open and closed W354 conformers. Upon ligand binding, the rate of WpD loop opening is very slow, while the rate

of loop closing likely remains rapid, resulting in a predominance of the WpD closed loop conformation. An alternative hypothesis in which the WpD loop remains open until closure is triggered by ligand binding is not supported by the present results.

ACKNOWLEDGMENT

We thank Dr. Janina Eads for critical reading of the manuscript and Dr. Colman Shannon for assistance with data analysis. We also wish to thank Dr. Marilyn Gunner for many helpful discussions.

REFERENCES

Asher, S. A., Ludwig, M., & Johnson, C. R. (1986) *J. Am. Chem. Soc. 108*, 3186−3197.
Austin, J., Jordan, T., & Spiro, T. (1993) in *Biomolecular Spectroscopy Part A* (Clark, R., & Hester, R., Eds.) pp 55−127, John Wiley and Sons, New York.
Bajzer, Z., & Prendergast, F. (1993) *Biophys. J. 65*, 3213−2323.
Barford, D., Flint, A. J., & Tonks, N. K. (1994) *Science 263*, 1397−1404.
Beechem, J., & Brand, L. (1985) *Annu. Rev. Biochem. 54*, 43−71.
Bolin, J., Filman, D., Matthews, D., Hamlin, R., & Kraut, J. (1982) *J. Biol. Chem. 257*, 13650−13662.
Bystroff, C., & Kraut, J. (1991) *Biochemistry 30*, 2227−2239.
Bystroff, C., Oatly, S., & Kraut, J. (1990) *Biochemistry 29*, 3263−3277.
Chang, M., Courtney, S., Cross, A., Gulotty, R., Petrich, J., & Fleming, G. (1985) *Anal. Instrum. 14*, 433−464.
Chen, L. X.-Q., Longworth, J., & Fleming, G. (1987) *Biophys. J. 51*, 865−873.
Chen, R., Knutson, J., Ziffer, H., & Porter, D. (1991) *Biochemistry 30*, 5184−5195.
Eckstein, J., Beer-Romero, P., & Berdo, I. (1996) *Protein Sci. 5*, 5−12.
Eftink, M. R., Selvidge, L. A., Callis, P. R., & Rehms, A. A. (1990) *J. Phys. Chem. 94*, 3469−3479.
Epstein, D., Benkovic, S., & Wright, P. (1995) *Biochemistry 34*, 11037−11048.
Farnum, M., Magde, D., Howell, E., Hirai, J., Warren, M., Grimsley, J., & Kraut, J. (1991) *Biochemistry 30*, 11567−11579.
Fodor, S. P. A., Copeland, R. A., Grygon, C. A., Spiro, T. G. (1989) *J. Am. Chem. Soc. 111*, 5509−5514.
Gerstein, M., Lesk, A., & Chothia, C. (1994) *Biochemistry 33*, 6739−6749.
Gottfried, D. S., Peterson, E. S., Sheikh, A. G., Yang, M., Wang, J., & Friedman, J.M. (1996) *J. Phys. Chem. 100*, 12034−12042.
Grinvald, A., & Steinberg, I. Z. (1974) *Anal. Biochem. 59*, 583−598.
Gryszynski, I., Eftink, M., & Lakowicz, J. (1988) *Biochim. Biophys. Acta 954*, 244−252.
Guan, K. L., & Dixon, J. E. (1990) *Science 249*, 553−556.
Guan, K. L., & Dixon, J. E. (1991) *J. Biol. Chem. 266*, 17026−17030.
Hansen, J., Rosenthal, S., & Fleming, G. (1992) *J. Phys. Chem. 96*, 3034−3040.
Harada, I., & Takeuchi, H. (1986) in *Spectroscopy of Biological Systems*; Clark, R. J. H., & Hester, R. E., Eds.; pp 113−175, John Wiley, New York.
Harada, I., Miura, T., & Takeuchi, H. (1986) *Spectrochim. Acta, Part A 42A*, 307−312.
Holtom, G. (1990) in *Time-Resolved Laser Spectroscopy in Biochemistry II*, Vol. 1204, SPIE.
James, D., Demmer, D., Steer, R., & Verral, R. (1985) *Biochemistry 24*, 5517−5526.
Johnson, M. L., & Frasier, S. G. (1985) *Methods Enzymol. 117*, 301−342.
Jordan, T., Eads, J., & Spiro, T. (1995) *Protein Sci. 4*, 716−728.
Lakowicz, J. (1984) in *Principles of Fluorescence Spectroscopy*, Plenum Press, New York.
Lipari, G., & Szabo, A. (1982a) *J. Am. Chem. Soc. 104*, 4546−4559.
Lipari, G., & Szabo, A. (1982b) *J. Am. Chem. Soc. 104*, 4559−4570.
Lolis, E., & Petsko, G. (1990) *Biochemistry 29*, 6619−6625.
Ludwig, M., & Asher, S. A. (1988) *J. Am. Chem. Soc. 110*, 1005−1011.
Miura, T., Takeuchi, H., & Harada, I. (1988) *J. Am. Chem. Soc. 27*, 88−94.
Miura, T., Takeuchi, H., & Harada, I. (1989) *J. Raman Spectrosc. 20*, 667−671.
Richmond, T. (1984) *J. Mol. Biol. 178*, 63−89.
Rodgers, K., Su, S., Subramaniam, S., & Spiro, T. (1992) *J. Am. Chem. Soc. 114*, 3697−1309.
Ruggiero, A., Todd, D., & Fleming, G. (1990) *J. Am. Chem. Soc. 112*, 1003−1014.
Schubert, H., Fauman, E., Stuckey, J., Dixon, J., & Saper, M. (1995) *Protein Sci. 4*, 1904−1913.
Stuckey, J., Schubert, H., Fauman, E., Zhang, Z.-Y., Dixon, J., & Saper, M. (1994) *Nature 370*, 571−575.
Szabo, A. (1984) *J. Chem. Phys. 81*, 150−167.
Szabo, A., & Rayner, D. (1980) *J. Am. Chem. Soc. 102*, 554−563.
Takeuchi, H., & Harada, I. (1986) *Spectrochim. Acta, Part A 42A*, 1069−1078.
Takeuchi, H., & Harada, I. (1990) *J. Raman Spectroscopy 21*, 509−515.
Takeuchi, H., Watanabe, N., Satoh, Y., & Harada, I. (1989) *J. Raman Spectrosc. 20*, 233−237.
Tao, T. (1969) *Biopolymers 8*, 609−632.
Waldman, A., Hart, K., Clarke, A., Wigley, D., Barstow, D., Atkinson, T., Chia, W., & Holbrook, J. (1988) *Biochem. Biophys. Res. Commun. 150*, 752−759.
Wierenga, R., Borchert, T., & Noble, M. (1992) *FEBS Lett. 307*, 34−39.
Williams, J. C., & McDermott, A. E. (1995) *Biochemistry 34*, 8309−8319.
Yguerabide, J., Epstein, H., & Stryer, L. (1970) *J. Mol. Biol. 51*, 573−590.
Zhang, Z.-Y., & Dixon, J. E. (1993) *Biochemistry 32*, 9340−9345.
Zhang, Z. Y., & Wu, L. (1997) *Biochemistry*, in press.
Zhang, Z.-Y., Clemens, J., Schubert, H., Stuckey, J., Fischer, M., Hume, D., Saper, M., & Dixon, J. (1992) *J. Biol. Chem. 267*, 23759−23766.
Zhang, Z.-Y., Wang, Y. Wu, L., Fauman, E., Stuckey, J. A., Schubert, H. L., Saper, M. A., & Dixon, J. E. (1994a) *Biochemistry 33*, 15266−15270.
Zhang, Z.-Y., Wang, Y., & Dixon, J. E. (1994b) *Proc. Natl. Acad. Sci. U.S.A. 91*, 1624−1627.

BI9622130